Predicting the Aerial Application of Dispersant Onto an Oil Spill

Milton E. Teske[1]
Continuum Dynamics, Inc.,
34 Lexington Avenue,
Ewing, NJ 08618
e-mail: milt@continuum-dynamics.com

Glen R. Whitehouse
Continuum Dynamics, Inc.,
34 Lexington Avenue,
Ewing, NJ 08618
e-mail: glen@continuum-dynamics.com

The release of dispersant from an aircraft onto an oil spill is simulated using the AGDISPpro computer model, to develop a better understanding of how aircraft type, spray systems, and meteorological conditions affect the prediction of surface deposition. This model, originally developed for predicting the aerial release of pesticides for agricultural spray applications, is ideally suited to simulate the effects of aircraft type and flight condition/configuration, spray system arrangement, wind speed and direction, temperature and relative humidity (evaporation), release height, and spray application rate when spraying an oil spill. Predictions of droplet trajectories from the aircraft to the surface, drop size distributions at the release height, and deposition profiles are compared to two historical datasets for the Lockheed C-130, from field studies conducted in 1982 and 1993. This article shows that model accuracy improves from $R^2 = 0.411$ to 0.827 with the earlier data, to $R^2 = 0.885$ to 0.968 with the later data, most probably because of a better understanding of nozzle locations in the 1993 data. Model accuracy also appears improved when the aircraft flies in an in-wind direction, a configuration strongly recommended in the available literature.
[DOI: 10.1115/1.4055984]

Keywords: computational fluid dynamics, mathematical modeling of fluid flows, modeling and simulation, simulation/physics-based modeling, sprays and droplets, turbulence

Introduction

Oil spills at sea represent a significant environmental challenge. The application of chemical dispersant to these spills enhances the dilution of the oil into smaller droplets so that the concentration of total hydrocarbons (within a given volume of seawater) quickly falls below toxicity thresholds. Floating oil represents a hazard to coastal life and all organisms frequently reaching the sea surface (e.g., dolphins and whales), while oil droplets represent a risk to most aquatic life and the flora and fauna (benthos) found on the bottom of the sea, as oil spill droplets—when diluted—tend to deposit on the sea floor.

Aerial delivery of dispersant is sensitive to an application procedure that must not only control the location of the deposited spray material but also its droplet size when the oil spill surface is reached. Dispersant deposition levels on the water surface, off-target airborne drift of the droplets, and dispersant evaporation when traveling from aircraft release to the water surface must also be considered. For example, dispersant droplets must be large enough to penetrate the oil layer but small enough to settle at the oil-water interface, with a typical thickness between 0.1 mm and 1.0 mm [1–8].

The first widely recognized use of an aircraft to spray damaging insects was published in 1922 [9]. Since then, significant progress has been made in the development of spray aircraft, understanding the potential and need for the aerial application of agricultural spray materials, the nozzles that deliver the spray materials accurately and efficiently, and the spray materials themselves. Numerical techniques have been developed and applied toward a better understanding of the mechanics of the spray process and their effect on the aerial release of spray material. It is prudent to consider how this development process has impacted the use of dispersant onto oil spills.

The first published use of aircraft in the oil spill problem can be traced to a field study where spray booms were placed on two aircraft, a Piper PA-25 Pawnee and a Douglas DC-4 [10]. Later field studies evolved toward larger fixed-wing aircraft, including the Douglas Aircraft DC-3 and DC-6, Canadair CL-215, and Lockheed C-130 [4], since oil spills generally occur far from shore, time is of the essence, and the size of the dispersant payload is therefore important. Helicopters were also investigated for shorter-range applications, including the MBB Bo 105, Sikorsky S61-N, and the Aérospatiale AS 330 Puma carrying buckets typically used for fighting forest fires.

For fixed-wing applications, the aircraft wake is represented by wingtip, flap, fuselage, and tail vortices, which play an important role in droplet breakup and the deposition pattern of the released dispersant on the water surface. Later publications suggest an evolving understanding of the role played by these vortices [3,11–15]. The initial development of the airborne dispersant delivery system (ADDS) and the later development of the modular aerial spray system (MASS) for the Lockheed C-130 provided two deposition datasets [3,14] spraying Corexit 9527 dispersant (Corexit Environmental Solutions LLC, Sugar Land, TX) to field study sites. These datasets provide the basis for the model application discussed herein.

Model History

In 1979, the National Aeronautics and Space Administration supported the initial development of AGricultural DISPersal (AGDISP), a Lagrangian-based droplet trajectory prediction model for the aerial application of pesticides. This modeling technology—with funding continued to 2020 by the USDA Forest Service—was made technically feasible by previous U. S. government-funded research undertaken by Continuum Dynamics, Inc. (CDI) and others, directed at understanding the physics of vortex wakes behind large commercial aircraft, particularly on takeoff and landing, behavior close to the ground where aerial spraying (pesticides or dispersants) is conducted [16,17]. The first published version of the model [18] was followed by subsequent model improvements and extensive comparisons to field data [19–21]. Additional model discussion and comparisons are reported in Refs. [22–29]. The latest model improvements and comparisons to data may be found in Ref. [30]. The AGDISP/AGDISPpro model is summarized in Appendix.

[1]Corresponding author.

Manuscript received August 28, 2022; final manuscript received October 8, 2022; published online November 11, 2022. Assoc. Editor: Esmail M. A. Mokheimer.

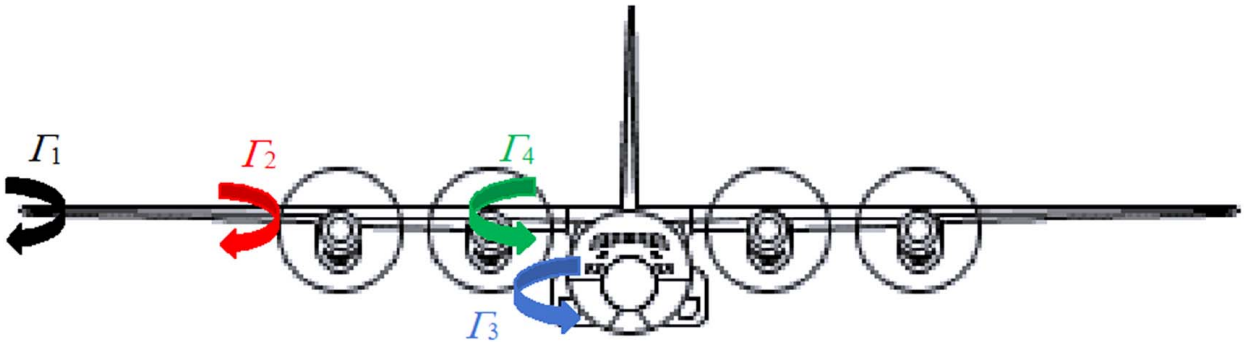

Fig. 1 The four trailed vortex pairs (shown on the right side of the aircraft only) from the Lockheed C-130 (schematic © fas.org): at the wingtip (Γ_1), the edge of the flaps (Γ_2), along the fuselage (Γ_3), and at the tail (Γ_4)

Methods

In aerial spray operations—whether pesticide sprays or oil dispersants—the dominant mechanism driving released material toward the ground is the induced flow field generated by the aircraft wake vortices (providing that the spray is not entrained by the engine wash). Flow field models for the Lockheed C-130, in both spraying configurations (ADDS and MASS), were developed following standard accepted practices and represented by trailed wake vortices from the wingtips, the wing flap edges, the aircraft fuselage, and the horizontal tail (Fig. 1) using the weighted components identified in Table 1 [31] and the physical characteristics compiled in Table 2. A description of each flow field and development of the corresponding Corexit 9527 drop size distributions follow.

Lockheed C-130 Flow Field Modeling. Reference [14] details a field study conducted in 1982 that included two days of testing, with a Lockheed C-130 flying at four heights and spraying Corexit 9527 dispersant through Tee Jet 6140 nozzle bodies (Spraying Systems, Glendale Heights, IL), without nozzle tips. Nozzles were positioned along two spray booms that extended from the open cargo bay, generating an effective boom width of 12.5 m (without nozzles across the open bay). This spray boom and nozzle configuration appear to form an initial version of ADDS [4,13,32]. Data collection included Kromekote cards for droplet size analysis and a sectioned trough for deposition.

A later field study [3,33] describes scoping studies that tested several methods for characterizing the swath width of Corexit 9527 sprayed from fixed-wing aircraft [34]. An extensive three-day set of field tests [3] examined the usage of the Lockheed C-130 and other aircraft. In these applications, Corexit 9527 was released through an initial version of MASS. This system included spray booms positioned below the trailing edges of the wings, near their tips, and spray booms extended through holes in the parachute doors [35]. Data collection included Mylar cards, monofilament and cotton strings, oil sensitive paper for droplet size analysis, metal trays, and a sectioned trough for deposition.

Point vortex theory [36] was used to track the behavior of the aircraft wake generated by the mutually induced movement of four vortex pairs (on the left and right sides of the aircraft) and their image vortices (used to simulate the surface) and were implemented into a modified version of AGDISPpro. Results—following the paths of the vortex centerlines from initiation to decay of the vortices—are shown in Figs. 2 and 3 for the two datasets. The 42% higher spraying speed in the 1993 data (Fig. 3) lowers the tip, flap, and tail vortex strengths equally, when compared to the 1982 data (Fig. 2) but increases the fuselage vortex strength. This change modifies the mutual vortical impact on the velocity field into which the dispersant was released.

The bluff-body flow effect induced at the rear of the cargo bay of the Lockheed C-130 (open in 1982, closed in 1993) generates additional vortical motion directly behind the aircraft [37–40]. Numerical simulations [41] computed an additional vertical velocity effect

Table 1 Fraction of aircraft weight carried by each component for a jet transport [31]

Component	Fraction of weight
Wing (with nacelles)	0.959
Fuselage	0.127
Tail	−0.086

Table 2 Lockheed C-130 spraying weight, spraying speed [14], and aircraft parameters (Lockheed Martin C-130 brochure, 2015)

Parameter	Value
Average aircraft weight	63,050 kg
Spraying speed	71.9 m/s
Wingspan	40.40 m
Span of flaps	24.16 m
Aircraft body diameter	4.40 m
Span of tail	16.06 m

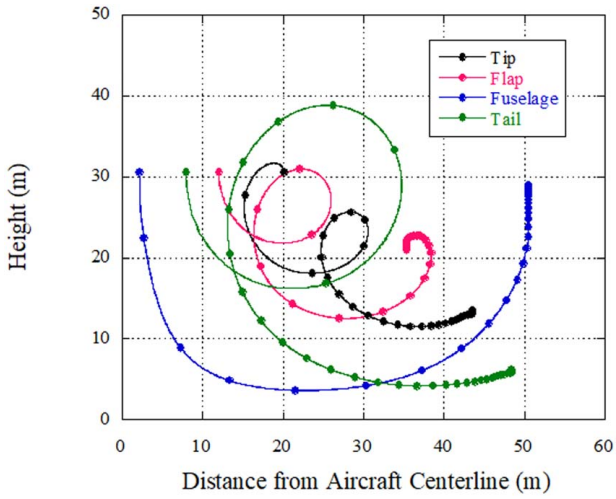

Fig. 2 The predicted time history behavior of the four vortices (on the right side of the aircraft) generated by the assumed spraying condition of the Lockheed C-130 in 1982, flying into the wind at an altitude of 30.5 m and a spraying speed of 71.9 m/s. The solid circles represent the location of the vortices at 10 s increments and tend to bunch up as the vortical strengths decay to zero.

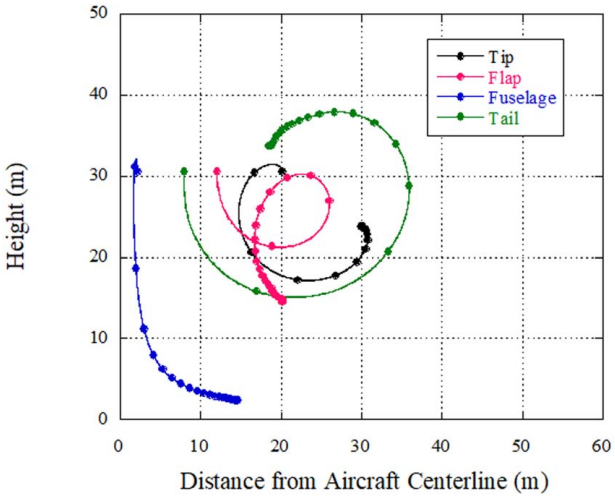

Fig. 3 The predicted time history behavior of the four vortices (on the right side of the aircraft) generated by the assumed spraying condition of the Lockheed C-130 in 1993, flying into the wind at an altitude of 30.5 m and spraying speed of 102.4 m/s. The solid circles represent the location of the vortices at 10 s increments and tend to bunch up as the vortical strengths decay to zero.

for over two chord lengths downstream of the cargo bay door, open or closed, confirmed with separate calculations [42] computing a consistent centerline vertical velocity greater than 9.0 m/s within the same distance downstream of the open bay door. This additional effect was assumed to increase the fuselage vortex strength and was included in the calculations discussed below.

Lockheed C-130 Drop Size Distributions. Simulating the release of spray material from the Lockheed C-130 requires an estimate of the initial drop size distribution (not measured by [14] or [3]) generated by the nozzles. Since the tips were removed from the Tee Jet 6140 nozzles in the 1982 test, it was assumed here that the nozzles acted as small-diameter tubes with a known cross-sectional area of 0.495 cm^2 [14]. To estimate this distribution, data on the effects of jet fuel jettisoned through exit ports on U. S. Air Force aircraft [43] were applied here. This study examined drop size distributions of water (as a substitute for jet fuel) at flow speeds comparable to dispersant discharge from the Lockheed C-130. Laser instrument readings (with a Sympatec LA-Helos^{TM}) were interpreted for the droplet diameters $D_{v0.1}$, $D_{v0.5}$, and $D_{v0.9}$ (μm), diameters below which droplets constitute 10%, 50%, and 90% of the total volume, respectively. Dimensional analysis [44–46] was applied to each of the three droplet diameters, scaled with the relative velocity between the tunnel air velocity U_{air} and the water jet velocity U_{jet} in m/s and nozzle area A (cm^2) based on the equation

$$D = a(U_{air} - U_{jet})^b A^c \tag{1}$$

where constants a, b, and c were found by least squares analysis (Table 3). Note that the power laws on relative velocity (constant b) averaged -2.305, consistent with the power law on Weber

Table 3 Modeling constants developed from wind tunnel test data

Droplet Size (μm)	a [μm (m/s)$^{-b}$/cm^{2c}]	b	c
$D_{v0.1}$	1.373×10^6	−2.498	0.228
$D_{v0.5}$	8.873×10^6	−2.413	0.150
$D_{v0.9}$	3.818×10^6	−2.005	0.125

Table 4 Computed droplet size comparisons for the Lockheed C-130 (1982 data). Equation (1) was used to develop the "Initial" droplet sizes summarized in the first row of the table. The "Final" droplet sizes average all AGDISPpro model predictions for the 1982 data

Distribution	$D_{v0.1}$ (μm)	$D_{v0.5}$ (μm)	$D_{v0.9}$ (μm)
Initial (average at the nozzle exit)	31.5	307.7	751.5
Final (average of release heights)	128.5	457.5	778.2

number scaling [47], where, for a specific value of Weber number, droplet diameter is inversely proportional to the square of the relative velocity.

Kromekote cards measured droplet sizes on the surface, while a sectioned deposition trough recovered deposition levels across the assumed swath width of 38 m. An average of the 22 trials found $U_{air} - U_{jet} = 67.5$ m/s. The field tests applied Corexit 9527. A NALCO Product Sheet (NALCO Environmental Solutions, Sugarland, TX, 2016) lists the evaporation rate of Corexit 9527 as 0.1 (water was referenced as 1.0). Since the dispersant was applied neat [4], predictions assumed that 10% of the released spray was volatile and used the quadratic evaporation rate of water [48] as a substitute for the evaporation rate of Corexit 9527.

The goal of the flight tests was to deposit $D_{v0.5}$ values between 350 μm and 500 μm. The average AGDISPpro prediction of $D_{v0.5}$ at the surface was 457.5 μm (Table 4). Model predictions recovered droplet diameters on the surface for dispersant released at three heights (9.1, 15.2, and 30.5 m) based on meteorological conditions (Table 5) estimated from historical records for the test location (Chandler, AZ) and dates (Nov. 3 and 4, 1982), as detailed meteorological data were not recorded by [14]. A logarithmic velocity profile was assumed for the wind speed between the dispersant release height and the ground.

Equation (1) was also applied to the 1993 data, with the averages finding $U_{air} - U_{jet}$ between 79.3 m/s and 92.0 m/s for the flights of interest. The initial droplet sizes for $D_{v0.1}$, $D_{v0.5}$, and $D_{v0.9}$ are shown in Table 6 (these droplet sizes are noticeably smaller than for the 1982 field studies). The goal of the 1993 flight tests was to have $D_{v0.5}$ values between 350 μm and 700 μm deposited on the surface [3]. Oil sensitive paper was used to measure droplet sizes.

Meteorological conditions (Table 5) were estimated from historical records for the test location and date, supplemented by additional data from Ref. [3] and the assumption of a logarithmic velocity profile.

The model predictions shown here include the effects of evaporation, removing on average 7.3% of the released spray for the eight Lockheed C-130 flights. Evaporation removes droplet sizes

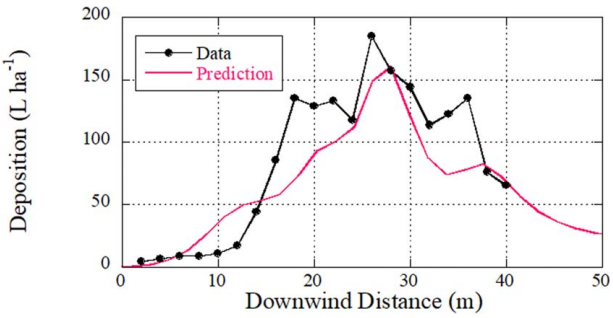

Fig. 4 Comparison of Flight A-3 model prediction (curve without dots) to ADDS deposition data [14] (curve with dots): 1590 l/min Corexit 9527 flowrate at a release height of 15.2 m. 84.8% of the released dispersant was captured by the sectioned trough. Model correlation with the trough data is $R^2 = 0.827$.

Table 5 Meteorological conditions estimated during the Lockheed C-130 spray trials outside Chandler, AZ (1982 data and www.almanac.com) and Alpine, TX (1993 data and www.almanac.com)

Parameter	Data (11/03/82)	Data (11/04/82)	Data (04/27/93)
Wind speed	3.50 m/s	1.29 m/s	3.86 m/s
Temperature	18.6 °C	17.4 °C	18.4 °C
Relative humidity	15.9%	17.9%	45.0%
Atmospheric pressure	1020 mb	1018 mb	1013 mb
Wet bulb temperature depression	10.83 °C	10.06 °C	6.61 °C

Table 6 Computed droplet size comparisons for the Lockheed C-130 (1993 data)

Distribution	$D_{v0.1}$ (μm)	$D_{v0.5}$ (μm)	$D_{v0.9}$ (μm)
Initial (average at nozzle exits)	17.1	170.4	459.4
Final (average on surface)	80.8	266.9	478.8

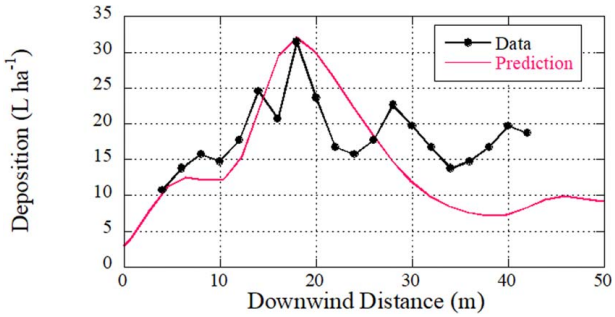

Fig. 5 Comparison of Flight B-6 model prediction (curve without dots) to ADDS deposition data [14] (curve with dots): 598 l/min Corexit 9527 flowrate at a release height of 30.5 m. Only 49.9% of the released dispersant was captured by the sectioned trough. Model correlation with the trough data is $R^2 = 0.411$.

across the original drop size distributions as the droplets descend to the surface.

Results and Discussion

Model predictions for both spraying configurations (ADDS and MASS) from data provided in Refs. [3,14], along with historical almanac meteorological data where necessary, are now described.

Lockheed C-130 With ADDS. Four ADDS deposition flights were plotted by Ref. [14]. This dataset raised the following modeling issues that required addressing:

(a) Meteorological conditions at the time of each flight were not reported, so almanac temperature and relative humidity values were assumed for evaporation effects. The absence of wind speed information required an assumption of the value of wind speed during each flight. A systematic evaluation was performed to iterate for the wind speeds that best located the horizontal position of the peak depositions recorded in each of the four flights, as shown in the model comparisons in Figs. 4–7. Photographs dated from 1982 clearly show dispersant streams released from each side of the aircraft by ADDS which, based on vortical effects, appear to combine into a single deposition peak (in Figs. 4, 5, and 7) and remain two peaks (in Fig. 6) by the time the ground was reached [4,49].

(b) Deposition was measured across a swath width of 38 m. Any deposition occurring outside this width was artificially added by Ref. [14] to the measured deposition by an "extended numerical approximation" to recover 100% of the released dispersant on the ground. With uncertainties present in this unexplained approach, only measured data within the swath are shown in the model comparisons in Figs. 4–7. Integrating the measured deposition data, multiplying by the aircraft speed (71.9 m/s), and dividing by the Corexit 9527 flowrates tabulated by [14] recovered the percentage of spray that was deposited within the 38 m swath and shown in these figures.

Predicted peak deposition levels correlate strongly with the data, but not when filling in the deposition on either side of the peaks. As will be shown through analysis of the second Lockheed C-130 dataset, these discrepancies are most likely due to assumptions regarding the locations of the spray boom and nozzles (approximated from available historical documents), and the complexities of the unsteady bluff-body flow field generated by the open cargo

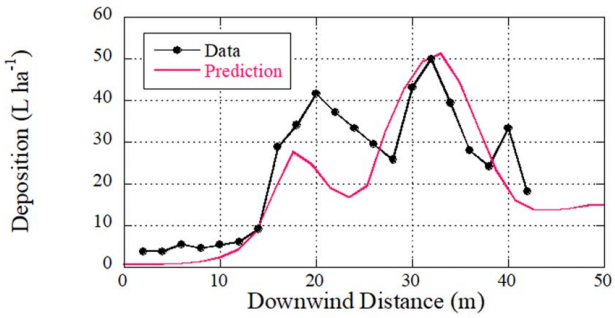

Fig. 6 Comparison of Flight B-9 model prediction (curve without dots) to ADDS deposition data [14] (curve with dots): 609 l/min Corexit 9527 flowrate at a release height of 9.1 m. 65.3% of the released dispersant was captured by the sectioned trough. Model correlation with the trough data is $R^2 = 0.734$.

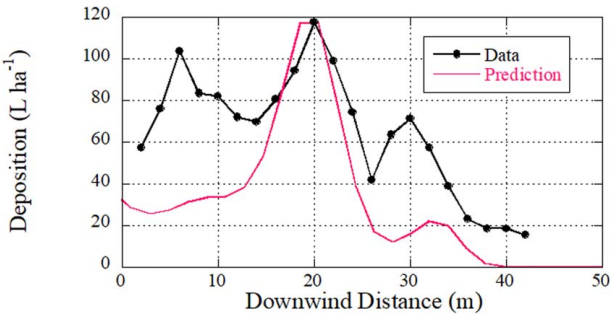

Fig. 7 Comparison of Flight B-10 model prediction (curve without dots) to ADDS deposition data [14] (curve with dots): 1295 l/min Corexit 9527 flowrate at a release height of 15.2 m. 85.3% of the released dispersant was captured by the sectioned trough. Model correlation with the trough data is $R^2 = 0.618$.

Table 7 Summary of model predictions for the 1982 data [14]. Tabulated values are referenced to the released dispersant as 100%. Deposition levels within the 38 m swath are shown in the second column; the other three columns report the complete model deposition predictions, the predicted drift downwind of the sectioned trough, and the corresponding evaporation levels

Flight	Predicted trough deposition (%)	Predicted total deposition (%)	Predicted total drift (%)	Predicted total evaporation (%)
A-3	74.0	94.1	0.0	5.9
B-6	49.1	83.5	9.6	6.9
B-9	68.8	84.1	10.4	5.5
B-10	51.8	81.7	12.3	6.0

bay door. The average coefficient of determination between the field data and model deposition predictions was $R^2 = 0.648$. Table 7 summarizes model predictions.

Lockheed C-130 With MASS. MASS deposition flights were grouped into four plots, each plot averaging the deposition measured from three flights, with data aligned with the maximum deposition level by [3]. As with the ADDS dataset, the 1993 dataset raised several modeling issues that required addressing:

(a) Meteorological conditions for 5 of the 12 flights were not measured; thus, predictions for these five flights assumed the corresponding almanac temperature and relative humidity values for evaporation effects. Since three flights were averaged for each plot, it made sense to iterate for the wind speeds that best located the horizontal position of the peak depositions recorded, as shown in the model predictions compared to data in Figs. 8–11.
(b) Integrating the measured deposition data, multiplying by the aircraft speed (102.4 m/s), and dividing by the Corexit 9527 flowrates tabulated by [3] recovered the percentage of spray that deposited within the trough and shown in these figures.
(c) Nozzle diameters were not reported in Ref. [3] and were assumed to be the same as in the 1982 flight tests.

These plots show significantly better agreement between model predictions and measured data (model predictions are summarized in Table 8). Note that the predicted evaporation levels are higher than in the 1982 dataset due to the higher release height in the 1993 dataset. The average coefficient of determination between the field data and model deposition predictions was $R^2 = 0.938$.

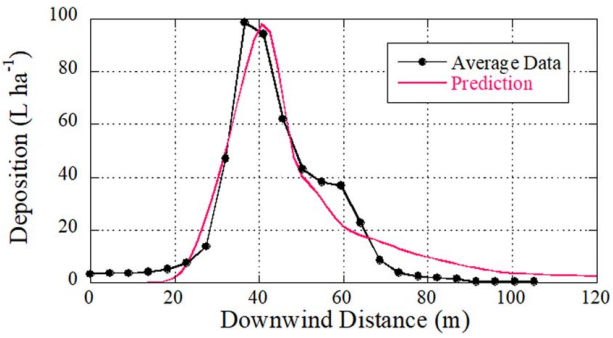

Fig. 8 Comparison of the average of Flights 16, 17, and 18 model predictions (curve without dots) to MASS deposition data [3] (curve with dots): 1567 l/min Corexit 9527 flowrate at a release height of 30.5 m. 90.5% of the released dispersant was captured by the sectioned trough. Model correlation with the trough data is $R^2 = 0.935$.

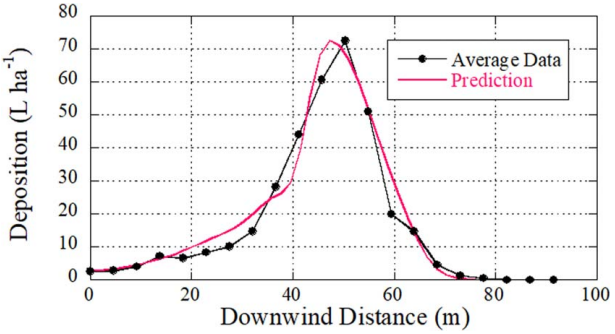

Fig. 9 Comparison of the average of Flights 19, 20, and 21 model predictions (curve without dots) to MASS deposition data [3] (curve with dots): 1293 l/min Corexit 9527 flowrate at a release height of 30.5 m. 77.0% of the released dispersant was captured by the sectioned trough. Model correlation with the trough data is $R^2 = 0.963$.

MASS Accountancy. Aerial application field tests and their modeling require an accounting of the destination of the spray material released from the aircraft, whether it be a water-based spray or Corexit 9527. Total accountancy and the environmental fate of these materials include predicting the evaporated vapor, ground and canopy deposition, and material aloft beyond the test area [50]. Tracking the evaporated vapor (up to 10% of the released

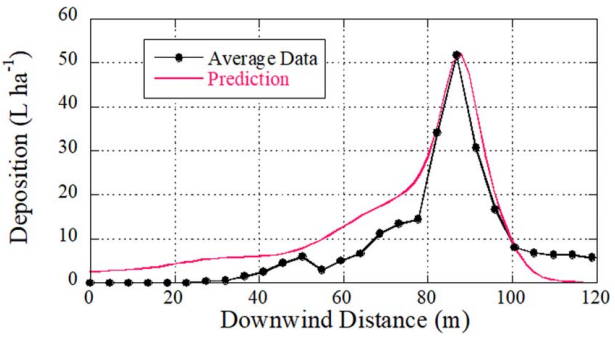

Fig. 10 Comparison of the average of Flights 22, 23, and 24 model predictions (curve without dots) to MASS deposition data [3] (curve with dots): 1293 l/min Corexit 9527 flowrate at a release height of 30.5 m. 54.5% of the released dispersant was captured by the sectioned trough. Model correlation with the trough data is $R^2 = 0.885$.

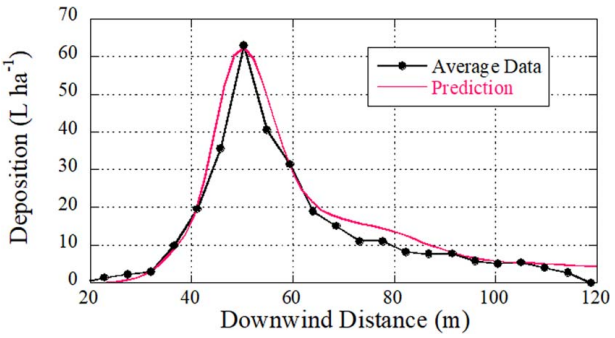

Fig. 11 Comparison of the average of Flights 25, 26, and 27 model predictions (curve without dots) to MASS deposition data [3] (curve with dots): 1399 l/min Corexit 9527 flowrate at a release height of 30.5 m. 62.2% of the released dispersant was captured by the sectioned trough. Model correlation with the trough data is $R^2 = 0.968$.

Table 8 Summary of model predictions for the 1993 data [3]. Tabulated values are referenced to the released dispersant as 100%. Deposition levels across the sectioned trough (91.4 m) are shown in the second column; the other three columns report the complete model deposition predictions, the predicted drift downwind of the trough, and the corresponding evaporation levels

Flights	Predicted trough deposition (%)	Predicted total deposition (%)	Predicted total drift (%)	Predicted total evaporation (%)
16, 17, 18	80.5	85.3	5.8	8.9
19, 20, 21	81.2	88.3	3.4	8.3
22, 23, 24	68.6	76.5	14.5	9.0
25, 26, 27	71.3	80.3	11.9	7.8

Table 9 Summary of average model predictions for Corexit 9527 spray released from the Lockheed C-130 (Figs. 4–7 for ADDS and Figs. 8–11 for MASS). There is little difference between the ADDS and MASS values, even though the average release height for ADDS was 17.5 m, compared to the release height for MASS of 30.5 m

Spray desposition	ADDS values (%)	MASS values (%)
Evaporation	6.1	8.5
Deposition	85.8	82.6
Downwind drift	8.1	8.9

dispersant in the case of Corexit 9527) accounts for the decrease in droplet sizes throughout the calculation, canopy deposition accounts for the removal of released dispersant by plant life, ground deposition (representing the deposit on ground collectors) recovers the dispersant pattern, and material aloft estimates what amount of dispersant is aloft beyond the ground collectors. This accountancy is summarized for the two Lockheed C-130 tests in Table 9. The higher MASS release height, compared to the average ADDS release height, results in an expected increase in evaporation, decrease in deposition, and increase in downwind drift. All calculations assumed a specific gravity of 1.0. Predictions not shown here suggest that small variations in specific gravity for Corexit 9527 did not affect the predicted results for either the ADDS or MASS systems.

Conclusions

Deposition results from spraying Corexit 9527 dispersant from Lockheed C-130 aircraft have been predicted with the AGDISPpro computer model. Predictions consistent with field measurements demonstrate the impact of crosswind effects on the peak and spread of the deposited material. AGDISPpro provides a physics-based model to enable a better understanding of the application of dispersant to oil spills. The behavior of dispersant—once it reaches the surface—may alter the average deposition level achieved by spraying, especially if the dispersant spreads rapidly from its predicted peak value to coat the oil spill surface at a more uniform deposition level.

Conflict of Interest

There are no conflicts of interest. This article does not include research in which human participants were involved. Informed consent not applicable. This article does not include any research in which animal participants were involved.

Data Availability Statement

The authors attest that all data for this study are included in the paper.

Appendix: AGDISPpro Model Equations

AGDISPpro tracks the motion of spray droplets released from nozzles positioned on a spray boom, with one droplet released from the center of each nozzle for each droplet size in the discretized drop size distribution. The Lagrangian approach followed here partitions the variables into mean and fluctuating components ($X_i + x_i$ for droplet location (m), $V_i + v_i$ for droplet velocity (m/s), and $U_i + u_i$ for background velocity (m/s), where the indices are not summed) to give the equations

$$\frac{d^2}{dt^2}(X_i + x_i) = [(U_i + u_i) - (V_i + v_i)]\left[\frac{1}{\tau_p}\right] + g_i \tag{A1}$$

$$\frac{d}{dt}(X_i + x_i) = (V_i + v_i) \tag{A2}$$

where t is time (s), X_i is the mean location of the droplet (m), x_i is the fluctuating location of the droplet (m), V_i is the mean velocity of the droplet (m/s), v_i is the fluctuating velocity of the droplet (m/s), U_i is the mean background velocity (m/s), u_i is the fluctuating background velocity (m/s), g_i is gravity (0, 0, $-g$) (m/s), and τ_p is the droplet relaxation time (s)

$$\tau_p = \frac{4}{3}\frac{\rho D}{C_D \rho_a |U_i - V_i|} \tag{A3}$$

where ρ is the droplet density (kg/m^3), D is the droplet diameter (μm), C_D is the droplet drag coefficient (non-dimensional), and ρ_a is the air density (kg/m^3). Equations governing the mean transport of a released droplet may then be written by ensemble averaging Eqs. (A1) and (A2)

$$\frac{d^2 X_i}{dt^2} = [U_i - V_i]\left[\frac{1}{\tau_p}\right] + g_i \tag{A4}$$

$$\frac{dX_i}{dt} = V_i \tag{A5}$$

The drag coefficient C_D in Eq. (A3) is evaluated empirically for spherical droplets [51] as

$$C_D = \frac{24}{\mathrm{Re}}[1 + 0.197\mathrm{Re}^{0.63} + 0.00026\mathrm{Re}^{1.38}] \tag{A6}$$

where the Reynolds number (non-dimensional) is defined as

$$\mathrm{Re} = \frac{\rho_a D |U_i - V_i|}{\mu_a} \tag{A7}$$

and μ_a is the viscosity of air (kg/m/s).

The fluctuation equations are obtained by subtracting Eqs. (A4) and (A5) from Eqs. (A1) and (A2), respectively, pre-multiplying appropriately by x_i and v_i, ensemble averaging and manipulating, to yield the equations

$$\frac{d}{dt}\langle x_i x_i \rangle = 2\langle x_i v_i \rangle \tag{A8}$$

$$\frac{d}{dt}\langle x_i v_i\rangle = [\langle x_i u_i\rangle - \langle x_i v_i\rangle]\left[\frac{1}{\tau_p}\right] + \langle v_i v_i\rangle \tag{A9}$$

$$\frac{d}{dt}\langle v_i v_i\rangle = 2[\langle u_i v_i\rangle - \langle v_i v_i\rangle]\left[\frac{1}{\tau_p}\right] \tag{A10}$$

These correlations represent $\langle x_i x_i\rangle$ as the position variance (m^2) around the mean droplet location X_i, $\langle x_i v_i\rangle$ as the correlation between droplet location and velocity (m^2/s), and $\langle v_i v_i\rangle$ as the droplet velocity variance (m^2/s^2), requiring the specification of $\langle x_i u_i\rangle$ and $\langle u_i v_i\rangle$, in Eqs. (A9) and (A10), correlations of the droplet location and velocity with the local background velocity, respectively, before solution is possible. The lengthy derivation for these correlations is not reproduced here but may be found in Ref. [19].

The droplet evaporation model was originally based on the diameter-squared law [52] in which the time rate of change of a droplet diameter is approximated by

$$\frac{dD}{dt} = -\frac{D}{2\tau_e\left[1 - \frac{t}{\tau_e}\right]} \tag{A11}$$

where τ_e is the evaporation time scale of the droplet (s)

$$\tau_e = \frac{2D_O^2}{\lambda \Delta\Theta \mathrm{Sh}} \tag{A12}$$

D_O is the initial droplet diameter (μm), λ is the evaporation rate ($\mu m^2/s/°C$), $\Delta\Theta$ is the wet bulb temperature depression (°C), and Sh is the Sherwood number, equal to $2(1 + 0.27\mathrm{Re}^{0.5})$. The evaporation rate is obtained by laboratory experiment and was initially set to 84.76 $\mu m^2/s/°C$ [53]. The wet bulb temperature depression is evaluated from the Carrier equation [54] and the saturation line in the steam tables [55]. Equation (A11) can be integrated to give

$$1 - \frac{D^2}{D_O^2} = \frac{t}{\tau_e} \tag{A13}$$

The evaporation model described by Eqs. (A12) and (A13) represents the evaporation of isolated droplets and assumes that every droplet in the released spray responds individually to ambient meteorological conditions, even though the spray nozzles eject streams of multiple droplets with multiple droplet sizes. The physics of the spray evaporation problem suggests that spray cloud effects play a significant role in evaporation. To this end recent laboratory tests idealized the effect of a spray cloud by stacking droplets on multiple threads, each thread positioned farther downwind of the thread ahead of it [48,56,57]. This thread configuration captures the near-neighbor droplet effects on droplet evaporation and acts as an indicator of the potential change in droplet evaporation when droplets form a spray cloud. In this way, the isolated evaporation rate is measured on droplets on the most upwind threads, and spray cloud effects on evaporation are measured on the most downwind threads (on droplets experiencing evaporation rates consistent with the evaporation of spray material released within a mini cloud of droplets from a spray nozzle). Results from this study extend the isolated droplet evaporation model to achieve a closer simulation of cloud effects, providing sufficient data to reach two conclusions: (1) a more appropriate representation of evaporation behavior for droplets inside a spray cloud is one that is quadratic in time; and (2) as the Reynolds number of the droplet decreases toward zero, the evaporation rate appears to decrease to one-half its isolated droplet value. These laboratory experiments suggested a more appropriate droplet evaporation model, replacing Eq. (A13) with

$$1 - \frac{D^2}{D_O^2} = a\frac{t}{\tau_e}\left[1 + b\frac{t}{\tau_e}\right] \tag{A14}$$

with the parameters $a = 0.2228$ and $b = 0.3136$ ($R^2 = 0.959$). The evaporation rate, for $\mathrm{Re} < 5$, can be expressed as

$$\frac{\lambda}{\lambda_O} = 0.5 + 0.27812\mathrm{Re} - 0.051249\mathrm{Re}^2 + 0.0031249\mathrm{Re}^3 \tag{A15}$$

where λ_O is the evaporation rate at $\mathrm{Re} > 5$ (with $R^2 = 0.554$), now set to 67.33 $\mu m^2/s/°C$ [57].

The Lagrangian trajectory model in AGDISPpro solves for the behavior of each droplet in the simulation, beginning at the nozzles on the spray boom and ending when the droplet either hits the ground or moves past the downwind edge of the assumed solution space. The equations described above are solved exactly with a sufficiently small time-step.

References

[1] National Research Council Committee on Effectiveness of Oil Spill Dispersants, 1989, *Using Oil Spill Dispersants on the Sea*, National Academy Press, Washington, DC.

[2] Sullivan, D., 1993, *Use of Chemical Dispersants for Marine Oil Spills*, U. S. Environmental Protection Agency, Office of Research and Development, Washington, DC, EPA/600/R-93/195.

[3] Giammona, C., Binkley, K., Fay, R., Denoux, G., Champ, M., Geyer, R., Bouse, F., Kirk, I., Gardisser, D., and Jamail, R., 1994, "Aerial Dispersant Application: Field Testing Research Program, Alpine, TX," MSRC Technical Report Series 94-019, Marine Spill Response Corp., Washington, DC.

[4] Fiocco, R. J., and Lewis, A., 1999, "Oil Spill Dispersants," Pure Appl. Chem., **71**(1), pp. 27–42.

[5] ASTM Standard Guide F1413, 2007, *Oil Spill Dispersant Application Equipment: Boom and Nozzle Systems*, ASTM International, West Conshohocken, PA, pp. 1–3.

[6] Canevari, J., Lindblom, G., Becker, K., Bowes, S., Brown, H., Cashion, B., Chen, A., Clark, J., Demarco, G., and Fiocoo, B., 2008, ExxonMobil Oil Spill Dispersant Guidelines. ExxonMobile Research and Engineering Company.

[7] Ebert, T. A., Downer, R., Clark, J., and Huber, C. A., 2008, "Summary of Studies of Corexit Droplet Impact Behavior Into Oil Slicks and Dispersant Droplet Evaporation," International Oil Spill Conference, Savannah, GA, May 4–8, American Petroleum Institute, 1, pp. 797-800.

[8] ITOPF Technical Information Paper No. 4, 2011, *Use of Dispersants to Treat Oil Slicks*, International Tanker Owners' Pollution Federation Ltd., London, UK, Paper No. 4, pp. 1–12.

[9] Neillie, C. R., and Houser, J. S., 1922, "Fighting Insects With Airplanes: An Account of the Successful Use of the Flying Machine in Dusting Tall Trees Infected With Leaf-Eating Caterpillars," National Geog. Mag., **41**(30), pp. 333–339.

[10] Cormack, D., and Parker, H., 1979, "The Use of Aircraft for the Clearance of Oil Spills at Sea," International Oil Spill Conference, Los Angeles, CA, Mar. 19–22, American Petroleum Institute, 1, pp. 469–473.

[11] Mackay, D., 1980, "Theoretical Assessment and Design Study of the Aerial Application of Oil Spill Dispersants," Environment Canada, Environmental Protection Service, Environmental Impact Control Directorate, Environmental Emergency Branch, Research and Development Division.

[12] Smedley, J. B., 1981, "Assessment of Aerial Application of Oil Spill Dispersants," International Oil Spill Conference, Atlanta, GA, Mar. 2–5, American Petroleum Institute, 1, pp. 253–257.

[13] Lindblom, G. P., and Cashion, B. S., 1983, "Operational Considerations for Optimum Deposition Efficiency in Aerial Application of Dispersants," International Oil Spill Conference, San Antonio, TX, Feb. 28–Mar. 3, American Petroleum Institute, 1, pp. 53–60.

[14] Lindblom, G. P., 1987, "Measurement and Prediction of Depositional Accuracy in Dispersant Spraying From Large Airplanes," International Oil Spill Conference, Baltimore, MD, Apr. 6–9, American Petroleum Institute, 1, pp. 325–328.

[15] Dillon-Gibbons, C., Galtry, C., Boustead, N., D'Arcy-Evans, N., Kurts, P., Jal, E., Kilner, A., and Washington, D., 2017, "Development of Oil Spill Response Decision Support Tool for Aerial Spraying of Dispersants," International Oil Spill Conference, Long Beach, CA, May 15–18, American Petroleum Institute, 1, pp. 725–744.

[16] Bilanin, A. J., Teske, M. E., and Williamson, G. G., 1977, "Vortex Interactions and Decay in Aircraft Wakes," AIAA J., **15**(2), pp. 250–260.

[17] Bilanin, A. J., Teske, M. E., and Hirsh, J. E., 1978, "Neutral Atmospheric Effects on the Dissipation of Aircraft Vortex Wakes," AIAA J., **16**(9), pp. 956–961.

[18] Bilanin, A. J., Teske, M. E., Barry, J. W., and Ekblad, R. B., 1989, "AGDISP: The Aircraft Spray Dispersion Model, Code Development and Experimental Validation," Trans. ASAE, **32**(1), pp. 327–334.

[19] Teske, M. E., Thistle, H. W., and Ice, G. G., 2003, "Technical Advances in Modeling Aerially Applied Sprays," Trans. ASAE, **46**(4), pp. 985–996.

[20] Teske, M. E., Thistle, H. W., and Londergan, R. J., 2011, "Modification of Droplet Evaporation in the Simulation of Fine Droplet Motion Using AGDISP," Trans. ASABE, **54**(2), pp. 417–421.

[21] Teske, M. E., Thistle, H. W., and Fritz, B. K., 2019, "Modeling Aerial Applied Sprays: An Update to AGDISP Model Development," Trans. ASABE, **62**(2), pp. 343–354.
[22] Bird, S. L., Perry, S. G., Ray, S. L., and Teske, M. E., 2002, "Evaluation of the AGDISP Aerial Spray Algorithms in the AgDRIFT Model," Environ. Tox. Chem., **21**(3), pp. 672–681.
[23] Teske, M. E., and Thistle, H. W., 2004, "Aerial Application Model Extension Into the Far Field," Biosys. Engr., **89**(1), pp. 29–36.
[24] Teske, M. E., Miller, P. C. H., Thistle, H. W., and Birchfield, N. B., 2009, "Initial Development and Validation of a Mechanistic Spray Drift Model for Ground Boom Sprayers," Trans. ASABE, **52**(4), pp. 1089–1097.
[25] Teske, M. E., Thistle, H. W., Schou, W. C., Miller, P. C. H., Strager, J. M., Richardson, B., Butler Ellis, M. C., Barry, J. W., Twardus, D. B., and Thompson, D. G., 2011, "A Review of Computer Models for Pesticide Deposition Prediction," Trans. ASABE, **54**(3), pp. 789–802.
[26] Teske, M. E., Thistle, H. W., and Kees, G. J., 2018, "Predicting Spray Drift From Backpack and UTV Spraying," Trans. ASABE, **61**(5), pp. 1559–1564.
[27] Teske, M. E., Wachspress, D. A., and Thistle, H. W., 2018, "Prediction of Aerial Spray Release From UAVs," Trans. ASABE, **61**(3), pp. 909–918.
[28] Teske, M. E., and Thistle, H. W., 2018, "The Influence of Forest Canopies on the Decay of Aircraft Wake Vortices and Downwash," Trans. ASABE, **61**(6), pp. 1857–1866.
[29] Thistle, H. W., Teske, M. E., Richardson, B., and Strand, T. M., 2020, "Technical Note: Model Physics and Collection Efficiency in Estimates of Pesticide Spray Drift Model Performance," Trans. ASABE, **63**(6), pp. 1939–1945.
[30] Teske, M. E., and Whitehouse, G. R., 2022, "Technical Note: AGDISPpro Model Comparisons With Additional Aerially Applied Deposition Data," J. ASABE (in preparation).
[31] Drela, M., 2011, "Development of the D8 Transport Configuration," 29th AIAA Applied Aerodynamics Conference, Honolulu, HI, June 27–30, pp. 3970–3983.
[32] Jefferies, J. C., and O'Neal, J., 1982, "Demonstration, Evaluation, and Physical Characterization of a Self-Contained Dispersant Spray System," American Petroleum Institute (API) Project Report.
[33] Fay, R. R., Giammona, C. P., Binkley, K., and Engelhardt, F. R., 1993, "Measuring the Aerial Application of Oil Dispersant From Very Large Aircraft at Moderate Altitude," EC/TDTS-94-02286-VOL 1-2, Proceedings of the 16th Arctic and Marine Oil Spill Program, Calgary, Alberta, Canada, June 7–9, pp. 1057–1063.
[34] Geyer, R., Faoy, R., Denoux, G., Giammona, C., Binkley, K., and Jamail, R., 1993, "Aerial Dispersant Application: Assessment of Sampling Methods and Operational Altitudes," Volume I, MSRC Technical Report Series 93-009.1, Marine Spill Response Corp., Washington DC.
[35] Lillie, T. H., 1988, "Contamination of the Exterior of a C-130E Aircraft Used for Aerial Spray," Air Force Occupational and Environmental Health Laboratory Report No. 88-137EQ0110JEF, Brooks AFB, TX.
[36] Batchelor, G. K., 2000, "An Introduction to Fluid Dynamics," *Cambridge Mathematical Library*, Cambridge University Press, Cambridge, pp. 583–591.
[37] Epstein, R. J., Carbonaro, M. C., and Caudron, F., 1994, "Experimental Investigation of the Flow Field About an Unswept Afterbody," J. Aircraft, **31**(6), pp. 1281–1290.
[38] Pinsky, H., Gray, M., Welch, M., and Yechout, T., 2009, Evaluation of the Drag Reduction Potential and Static Stability Changes of C-130 Aft Body Strakes," AIAA 2009-1721, Albuquerque, NM.
[39] Schmidt, S., 2010, "Detached-Eddy Simulation of the Dynamic Loads of C-130H With Open Cargo Bay," 17th Australasian Fluid Mechanics Conference, Auckland, NZ, Dec. 5–9.
[40] Bergeron, K., Ghoreyshi, M., and Jirasek, A., 2018, "Simulation of C-130 H/J Troop Doors and Cargo Ramp Flow Fields," Aerospace Science Tech., **72**, pp. 525–541.
[41] Ghoreyshi, M., Bergeron, K., and Lofthouse, A. J., 2018, "Numerical Simulation of Wake Flow Field Behind the C-130 With Cargo Ramp Open," J. Aircraft, **55**(3), pp. 1103–1121.
[42] Robertson, C. D., 2019, "A Computational and Design Characterization for the Flow Field Behind a C-130 During an Unmanned Aerial Vehicle Docking," Master of Science dissertation, The Ohio State University, Columbus, OH.
[43] Teske, M. E., Kaufman, A. E., and Polymeropoulos, C. E., 1996, "Drop Size Distribution From Large Orifices," ILASS-Americas 9th Annual Conference on Liquid Atomization and Spray Systems, San Francisco, CA, May 19–22, pp. 268–272.
[44] Marshall, W. R., 1954, "Atomization and Spray Drying," American Inst. Chem. Eng., Chem. Eng. Prog. Monogr. Ser., **50**(2), p. 122.
[45] Weiss, M. A., and Worsham, C. H., 1959, "Atomization in High Velocity Airstreams," J. Am. Rocket Soc., **29**(4), pp. 252–259.
[46] Adelberg, M., 1968, "Mean Drop Size Resulting From the Injection of a Liquid Jet Into a High-Speed Gas Stream," AIAA J., **6**(6), pp. 1143–1147.
[47] Lasheras, J. C., Villermaux, E., and Hopfinger, E. J., 1998, "Break-Up and Atomization of a Round Water Jet by a High-Speed Annular Air Jet," J. Fluid Mech., **357**, pp. 351–379.
[48] Teske, M. E., Thistle, H. W., Riley, C. M., and Hewitt, A. J., 2018, "Laboratory Measurements of Evaporation Rate of Droplets at Low Relative Wind Speed," Trans. ASABE, **61**(3), pp. 919–923.
[49] Fingas, M., 2011, "A Practical Guide to Chemical Dispersion for Oil Spills," *Oil Spill Science and Technology*, M. Fingas, ed., Gulf Professional Publishing, Houston, TX, pp. 583–610.
[50] Teske, M. E., Barry, J. W., and Thistle, H. W., 1995, "Environmental Fate and Accountancy," *Chapter 7 of Biorational Pest Control Agents: Formulation and Delivery*, F. R. Hall, and J. W. Barry, American Chemical Society Symposium Series No. 595, American Chemical Society, Washington, DC, pp. 95–107.
[51] Langmuir, I., and Blodgett, K. B., 1949, "A Mathematical Investigation of Water Droplet Trajectories," Report No. RL225, General Electric Company, Schenectady, NY.
[52] Trayford, R. S., and Welch, L. W., 1977, "Aerial Spraying: A Simulation of Factors Influencing the Distribution and Recovery of Liquid Droplets," J. Agric. Engr. Research, **22**(2), pp. 183–196.
[53] Fuchs, N. A., 1959, *Evaporation and Droplet Growth in Gaseous Media*, Pergamon Press, New York, pp. 38–59.
[54] Jennings, B. H., and Lewis, S. R., 1950, *Air Conditioning and Refrigeration*, International Textbook Company, Scranton, PA, pp. 48–51.
[55] Meyer, C. A., McClintock, R. B., Silvestri, G. J., and Spencer, R. C., 1979, *ASME Steam Tables—Thermodynamic and Transport Properties of Steam*, 4th ed., ASME, New York, NY.
[56] Teske, M. E., Thistle, H. W., Riley, C. M., and Hewitt, A. J., 2016, "Initial Laboratory Measurements of the Evaporation Rate of Droplets Inside a Spray Cloud," Trans. ASABE, **59**(2), pp. 487–493.
[57] Teske, M. E., Thistle, H. W., Riley, C. M., and Hewitt, A. J., 2017, "Laboratory Measurements on the Sensitivity of Evaporation Rate of Droplets Inside a Spray Cloud," Trans. ASABE, **60**(2), pp. 361–366.